Desalination and Water Treatment
www.deswater.com
doi: 10.5004/dwt.2022.28104

248 (2022) 176–187
February

Decontamination of copper(II) from aqueous solutions using synthesized polyaniline/montmorillonite composite

Adel A. El-Zahhar[a,b,*], Mutasem Z. Bani-Fwaz[a], Ismat H. Ali[a], Riadh Marzouki[a]

[a]*Chemistry Department, College of Science, King Khalid University, P.O. Box: 9004, Abha 61413, Saudi Arabia, emails: elzahhar@kku.edu.sa (A.A. El-Zahhar), mbanifawaz@kku.edu.sa (M.Z. Bani-Fwaz), ihali@kku.edu.sa (I.H. Ali), rmarzouki@kku.edu.sa (R. Marzouki)*
[b]*Nuclear Chemistry Department, Hot Labs Center, AEA, Cairo – 13759, Egypt*

Received 10 September 2021; Accepted 29 December 2021

ABSTRACT

The adsorptive removal of copper(II) ions from aqueous solutions were studied using the prepared polyaniline/montmorillonite composite adsorbent. The controlling parameters as: pH, adsorbent dose, ion concentration and temperature were studied. The removal of Cu(II) reached its maximum value at pH 5.5 and the equilibrium adsorption capacity was found to be 99.61 mg g^{-1} on the composite adsorbent. The experimental adsorption results were found to follow Langmuir adsorption isotherm model with maximum adsorption capacity of 100.01 mg g^{-1}. The kinetic studies showed good fit of the experimental results with pseudo-second-order kinetic model, indicating the participation chemisorptions.

Keywords: Decontamination; Copper(II); Polyaniline; Montmorillonite; Composite

1. Introduction

Polymer composites containing layered silicates have found great attention due to their advanced properties [1]. The layered silicates were studied in many applications and were involved in many techniques due to their surface properties and layer charges [2]. The reaction between clay particles and polymeric materials are highly dependent on the hydroxyl groups and surface layer charges in the clay particle. Polymer-clay composite systems could be formed through clay intercalation or exfoliation. If nano-sized clay particles were used in polymer composites; polymeric moieties could be intercalated within the clay interlayer and between platelets. While if the clay platelets are dispersed within the polymeric chains, it is called exfoliation. The most effective clay properties that could improve the composite properties include clay particle size, surface area, and clay aspect ratio [3]. Montmorillonite (MMT), smectite clay minerals which have advanced intercalation characteristics, strong adsorption and higher affinity towards metal ions as a result of its layered structure [4]. MMT has wide advanced applications due to its high cation exchange capacity, high surface area, high aspect ratio and distinctive layered structure. MMT has been studied for the removal of hazardous heavy metal ions as; As, Cd, Cr, Co, Cu, Fe, Pb, Mn, Ni, and Zn [5]. The metal ions adsorption behavior of MMT was found to be highly enhanced via certain modifications as; inclusion polymeric composites, grafting, impregnation, chelation and crosslinking [6]. The polymer-clay composite adsorbents have been prepared for

* Corresponding author.

the sake of enhancing adsorption selectivity, regeneration behavior, surface area and surface morphology [7,8].

Different conductive polymers have important studies in metal ions adsorption as polypyrrole, polyaniline (PANI), polythiophene, and polyfuran [9]. PANI has prominent characteristic properties as electrochemical properties, amine functionality, high environmental stability, low cost and characteristic doping behavior. These properties make PANI applicable in metal ions adsorption however it has low swelling properties which limited its applications in water treatment. However many approaches have been studied for overcoming these limitations as blending with nanosized two-dimensional materials [1]. The dispersion of monomer molecules within the clay platelets aggregate with controlled level provide intercalated or exfoliated polymer clay composite with highly enhanced properties [10]. The polymer clay nanocomposites were reported as efficient adsorbent for wastewater treatment with low cost [11].

Copper(II) ions were found with significant amounts in certain industrial wastes as: metal finishing, electroplating, mining industries plastics, batteries, and etching [12,13].

Copper ions has been known with their harmful effect on the environment and human health, where high copper intake in human body produce serious health effect as cramps, vomiting, convulsions and in some cases it could causes death [14–16]

The United States Environmental Protection Agency (USEPA) has limited the permissible copper ions concentrations in industrial discharge to be 1.3 mg L^{-1}. While, copper ions concentration in drinking water was limited by the World Health Organization to be less than 2 mg L^{-1} [17].

Different methods and materials were studied for removal of copper ions from wastewater as: adsorption [18], membrane filtration [19,20], electrodialysis [21] and photocatalysis [22]. Adsorption process has been widely applied for effective removal of copper from wastewater due to simple performance, high efficiency and low coast [23]. Tea agricultural waste was studied for adsorption Cu(II) ions from aqueous solution and the results indicated that 74% of the copper ions were removed [24]. The removal of copper ions from aqueous solutions using *Azadirachta indica* (neem leaf) powder was studied and the highest removal of copper ions was obtained at pH 7.0 [25]. Trans-cinnamic acid was synthesized and studied for removal of copper ions from wastewater and the results showed maximum adsorption capacity of 389.3 mg g^{-1} [26]. The lignocellulosic fractions of Q. ilex and Q. suber were studied for copper ions adsorption from aqueous solutions and showed experimental adsorption of 48.06 and 38.19 mg g^{-1}, respectively [27]. The removal of copper ions from aqueous solutions was studied using polymeric adsorbents and the results showed significantly improved adsorption by using polymer nano-composite adsorbents [28]. PANI coated surface sawdust was prepared and studied for Cr(VI) ion [29], while PANI-CuO nanocomposite was prepare through chemical coprecipitation and studied as microwave shielding material [30]

Different method and procedures have been used for preparation of PANI and PANI composites. The produced PANI composites were potentially studied for many applications as providing water solubility, fabrication of PANI thin film nanocomposite and charge storage applications. The PANI composites were prepared through different methods as interfacial polymerization, layer by layer assembly, coating and doping. It has been reported that the properties of PANI composites are clearly dependent on the preparation procedure [31].

PANI nanocomposites have been potentially studied for heavy metals adsorption and offered improved adsorption efficiency if compared with individual materials [32]. Polyaniline doped with Mn_2O_3 has been prepared [33] and studied for the adsorption of Pb(II), Cd(II), and Ni(II) ions and showed maximum adsorption capacity of 437, 480, and 494 mg g^{-1}, respectively. The fast chelation mechanism was observed in the adsorption process. PANI/Sb_2O_3 composite was prepared through in situ polymerization process [34] and applied for the adsorption of Pb(II) from aqueous solutions. The adsorption of Pb(II) using PANI/Sb_2O_3 was found to be affected by solution pH and the maximum adsorption capacity was found to be 21.05 mg g^{-1}. The main adsorption mechanisms responsible for the adsorption process include ion exchange and surface complexation. The adsorption behavior of heavy metal ions using the prepared Al_2O_3/PANI nanocomposite was studied and showed the metal ions affinity order of Cu^{2+}, $Pb^{2+} > Zn^{2+} > Cd^{2+} > Ni^{2+}$, Co^{2+} [35]. The prepared nanocomposite offered a nanofibrous and nanoporous structure with pore diameter in the ranging within 70–100 nm.

Different PANI based composites were prepared and studied for removal of organic pollutants and showed considerable removal efficiency. Polyaniline based almond shell biocomposite PANI/AS was prepared and studied for the removal of organic G dye from aqueous solution [36]. The adsorption results of OG dye by PANI/AS was found to be fitted with the pseudo-second-order kinetic model and followed the Freundlich isotherm model with maximum adsorption capacity of 190.98 mg g^{-1}.

The adsorption of anionic dye eosin yellow (EY) from aqueous solution was studied using PANI/Emeraldine salt [37]. The adsorption results of EY showed good fitting with pseudo-second-order kinetic model and the maximum adsorption capacity was found to be 335 mg g^{-1}. PANI/Sawdust has been prepared [38] and applied for adsorption of aromatic acids with good adsorption efficiency. The maximum adsorption capacity of polyaniline/*Argan*-nut-shell composite was observed to be 209.64, 143.68 and 267.38 mg g^{-1} for Tri, Hemi and Pyro acids, respectively.

In this context, polymer-clay composite adsorbent was prepared from polyaniline (PANI) and montmorillonite (MMT). The prepared composite PANI/MMT was analyzed for assigning the physicochemical, structural and surface properties and studied for the removal of Cu(II) ions from aqueous solutions. The parameters affecting the adsorption of Cu(II) onto PANI/MMT were studied and the adsorption mechanism was suggested based on isothermal and kinetic studies.

2. Experimental

2.1. Materials

MMT was purchased from Sigma-Aldrich, aniline was obtained from Fluka and ammonium persulfate (APS) was purchased from Sigma-Aldrich. Copper sulfate was obtained from Sigma-Aldrich.

2.2. Synthesis of the composite PANI/MMT

Different synthetic routes have been studied for preparation of PANI composite based on three main procedures [32]:

- In situ polymerization of aniline monomer onto the surface of nanoparticles.
- Simultaneous polymerization and nanoparticles formation in One-Step redox reactions
- Mixing of the pre-synthesized PANI and nanomaterials.

Sun et al. [39] studied the preparation of Fe_3O_4/PANI nanocomposite through microemulsion polymerization process of Fe_3O_4 and aniline monomer. The obtained Fe_3O_4/PANI composite showed a monodispersed core–shell structure and superparamagnetic properties. Multi walled carbon nanotube polyaniline composite MWCNT/PANI has been prepared through microemulsion process using APS as initiator [40]. Different PANI composites were also prepared through inverse emulsion polymerization process for monomer aqueous solution emulsified in non polar organic solvent. This process showed many advantages as ease of process control due to the physical state of the emulsion system. PANI/TiO_2 nanocomposite has been prepared using CTAB as an emulsifier [41] and showed average diameter between 50–200 nm. Nanocomposite of PANI/GO was synthesized via dynamic interfacial inverse emulsion polymerization process using APS as initiator [42]. Wang et al. [43] synthesized PANI/TiO_2 composite via one-pot synthesis process, where TiO_2 was prepared firstly followed by aniline polymerization using APS as initiator. The prepared composite showed core–shell morphological structure of PANI covering TiO_2.

The composite adsorbent PANI/MMT was prepared through chemically initiated polymerization of aniline in presence of MMT particles. The process applied for PANI/MMT composite preparation was facile, productive and produces adsorbent particles with considerable granular appearance as well. Briefly, the appropriate amount of MMT (to give MMT content ratio of 20) was suspended in distilled water at 25°C, the aniline monomer (3 g) was added to the MMT suspension and left for 24 h under continuous stirring to verify intercalation within MMT. The APS solution of (5.71 g in 25 mL distilled water) was added to the reaction mixture with continuous stirring for 5 h till complete polymerization. The solid composite PANI/MMT was collected and rinsed with 0.2 mol L^{-1} HCl solution and dried at ambient till complete dryness.

The conversion yield was calculated gravimetrically by the following equation:

$$\text{Conversion yield} = \frac{M_o - M_1}{M_2} \tag{1}$$

where M_o, M_1 and M_2 are the prepared composite mass, MMT mass, and the starting aniline mass, respectively.

2.3. Characterization of the prepared materials

The characteristic surface properties (specific surface area and pore size) of the prepared composite adsorbent and polymer were analyzed by N_2 adsorption using Belsorp surface area analyzer (BEL Japan, Inc.). The specific surface areas were determined using Belsorp Adsorption/Desorption Data Analysis Software.

Fourier-transform infrared (FT-IR) spectra of MMT, PANI and PANI/MMT were analyzed within the wavenumber range of 4,000–400 cm^{-1} using Thermo Scientific Nicolet 6700 FT-IR. The X-ray diffraction (XRD) patterns of MMT, PANI and PANI/MMT were analyzed using Shimadzu 6000DX instrument (Shimadzu Corporation, Japan), operated at 40 kV, 30 mA, and λ = 0.154056 nm. The thermal stability of MMT, PANI and PANI/MMT were studied using a Shimadzu TGA-50H thermogravimetric analyzer (TGA), where the samples were heated from ambient to 800°C with heating rate of 15°C/min under nitrogen flow of 40 mL min^{-1}.

The surface morphology of the prepared composite and polymer were studied by scanning electron microscopy (SEM) using FESEM with Jeol Model 6360 LV SEM (USA).

2.4. Adsorption study of Cu(II)

Batch adsorption experiments were performed where, the adsorption efficiency was studied depending on pH of Cu(II) aqueous solution, contact time, adsorbent dose and Cu(II) ion concentration. The Cu(II) aqueous solutions was prepared from $CuSO_4{\cdot}5H_2O$ to obtain Cu(II) concentrations within 50–250 mg L^{-1}. The adsorbent amount of 0.1 g was transferred to the reaction vial containing 50 mL of Cu(II) aqueous solution and agitated in thermostat-water bath shaker at 150 rpm and the temperature was fixed at 25°C ± 1°C. The removal percentage of Cu(II) (R %) was calculated as:

$$R\% = \frac{C_o - C_e}{C_o} \times 100 \tag{2}$$

where C_o and C_e are the initial and equilibrium concentrations of Cu(II) (mg L^{-1}) in solution, respectively. The adsorbed amount of Cu(II) on the solid adsorbent (q, mg g^{-1}) was calculated as:

$$q = \left(C_o - C_e\right) \times \frac{V}{m} \tag{3}$$

where V is the Cu(II) solution volume (L) and m is the adsorbent mass (g). The pH of aqueous solution was adjusted using 0.1 M HCl and 0.1 M NaOH solutions as required. The mixing time was varied from 5 to 180 min. The Cu(II) concentration before and after experiments was measured using atomic absorption spectroscopy.

2.5. Regeneration–recycling

The regeneration of the Cu(II) loaded adsorbent was studied by shacking the Cu-loaded adsorbent in 0.1 M HCl solution for 30 min, then washing with distilled water.

The regenerated particles were applied in repeated adsorption–desorption–regeneration cycles and the efficiency of the regenerated adsorbent was calculated as in Eq. (1).

3. Results and discussion

3.1. Characterization of the prepared materials

The conversion yield of aniline to PANI was found to be 71.5%, which is slightly lower than the previously reported yield [44]. This finding could be due to the possible aggregation of MMT particles, which could affect the monomer swilling and stability. Furthermore, the MMT content increases the viscosity of the reaction mixture, which could affect the monomer conversion yield.

The surface analysis results revealed that PANI/MMT and PANI have surface area of 98.21 and 29.51 $m^2\ g^{-1}$, respectively. The pore volume for PANI/MMT and PANI was found to be 0.45 and 0.20 $cm^3\ g^{-1}$, respectively. These results indicate the improved surface area and pore size by inclusion of MMT with PANI. The composite pore size for PANI/MMT was found to be 374.1 Å, compared with 288.1 Å for PANI. The surface analysis results reflect the possible increase in the available surface active sites on PANI/MMT which could improve both the metal ions adsorption and diffusion within composite layers. The prepared composite particles were sized to be within 1–2 mm for adsorption experiments.

The FT-IR spectra of PANI, MMT and PANI/MMT composite with 20 wt.% MMT are presented in Fig. 1a. The characteristic peaks in PANI spectrum appeared at 1,610 and 1,460 cm^{-1} could be assigned for the stretching vibration of C=N and C=C, respectively [45]. The peak appeared at 1,297 cm^{-1} could be assigned for stretching vibration of C–N, where the peaks at 1,107 and 798 cm^{-1} could assigned for the out-of-plane bending of C–H of the rings. The MMT spectrum showed the peaks at 1,051 and 520 cm^{-1}, which could be assigned for Si–O and Al–O stretching vibrations, respectively [46]. The presence of the characteristic peaks for both MMT and PANI prove the formation of the composite PANI/MMT. There is a slight shift in characteristic peaks position of MMT and PANI in the composite compared to their original peaks in pure compounds. The characteristic peak for Si–O stretching vibration at 1,051 cm^{-1} in PANI/MMT spectrum and the peak of C–H out-of-plane bending at 1,107 cm^{-1} appeared in PANI/MMT spectrum with broadening, indicating the presence of certain interaction between MMT and PANI.

The thermogravimetric analysis (TGA) of PANI/MMT, PANI and MMT is presented in Fig. 1b and shows a small weight loss at about 90°C in MMT curve due to loss of moisture. The second-step in MMT thermal degradation appeared between 250°C–600°C, corresponding to the dehydroxylation and decomposition of organics in MMT. The thermogravimetric analysis of PANI showed two degradation steps, the first one at 240°C and the second was at 440°C. Where the TGA of PANI/MMT composite with 20 wt.% MMT, showed weight loss at 230°C assigned for dehydroxylation of MMT and dehydration of interlayer water, the second-step at 440°C assigned for the decomposition of organic moieties within the MMT layers, and the third step was appeared at 555°C for the PANI polymer backbone degradation. The thermal analysis results reflect the improved thermal stability of PANI in presence of MMT, which agreed with the previously reported results [47]. The increased thermal stability of PANI with presence of MMT could be explained as MMT sheets worked as permeation/diffusion barriers which hindered the diffusion of gaseous products within the composites and inhibit PANI thermal decomposition [48].

XRD analysis patterns of MMT, PANI and PANI/MMT are given in Fig. 1c and reveal that the dominant peak of MMT at $2\theta = 26.6°$ corresponding a basal spacing of 3.35 Å. The PANI/MMT composite XRD pattern in Fig. 1c shows slight shift peaks positions and decreased peaks intensities compared to MMT pattern. The peaks appeared at lowered angels reflect the intercalation of PANI within MMT and declare the increased interlayer distance of MMT due the formation of intercalated composite structure. This explanation could be supported by the possible interaction of the polymer amine groups with MMT silicate groups, which could greatly enhances the formation stacked PANI/MMT composite [49,50]. The MMT peaks intensities decreased due to low MMT content within the composite, while the peaks broadening may be due to the hydration of MMT cations and the changed layer spacing which also confirms the presence of intercalated structure.

The surface morphology of PANI and PANI/MMT was analyzed by SEM and the micrographs are given in Fig. 1d. The SEM micrographs show the layers of MMT and the PANI spheres within the clay. Certain agglomeration of PANI spheres was observed and separate layers of MMT with certain stacking due to its higher content and polymer intercalation within the layer spacing [44].

3.2. Adsorption study of Cu(II)

3.2.1. Effect of pH

The aqueous solution pH has significant effect on adsorption of metal ions from aqueous solutions. The effect of pH on the adsorption of Cu(II) on PANI and PANI/MMT was studied within pH range 1–7, at 25°C ± 1°C, adsorbent dose of 2 g L^{-1}, contact time of 60 min and Cu(II) ion concentration of 200 mg L^{-1}. The results given in Fig. 2a show increased removal percentage of Cu(II) ions onto PANI or PANI/MMT with increasing pH from 1 to 5. However, further increase in pH from 5 to 7 resulted in decrease in Cu(II) adsorption. Therefore, pH 5.5 was considered as the optimum for the adsorption of Cu(II) in all experiments. These results could be explained by the surface charge variation of the adsorbent with pH, where at lower pH the surface sites are protonated, and the adsorbent surface tends to be positively charged, consequently the electrostatic interaction is low and the adsorption of Cu(II) is low. While, as the pH increased up to 5, the surface sites are deprotonated and the adsorbent active sites tend to be negatively charged, the electrostatic interaction could be effective, and the adsorption increases. As the pH increased near the alkaline, the bonding between Cu(II) and the PANI/MMT increased. Also the de-protonation of the polymer amine groups at high pH increases the active boding sites available for Cu(II)

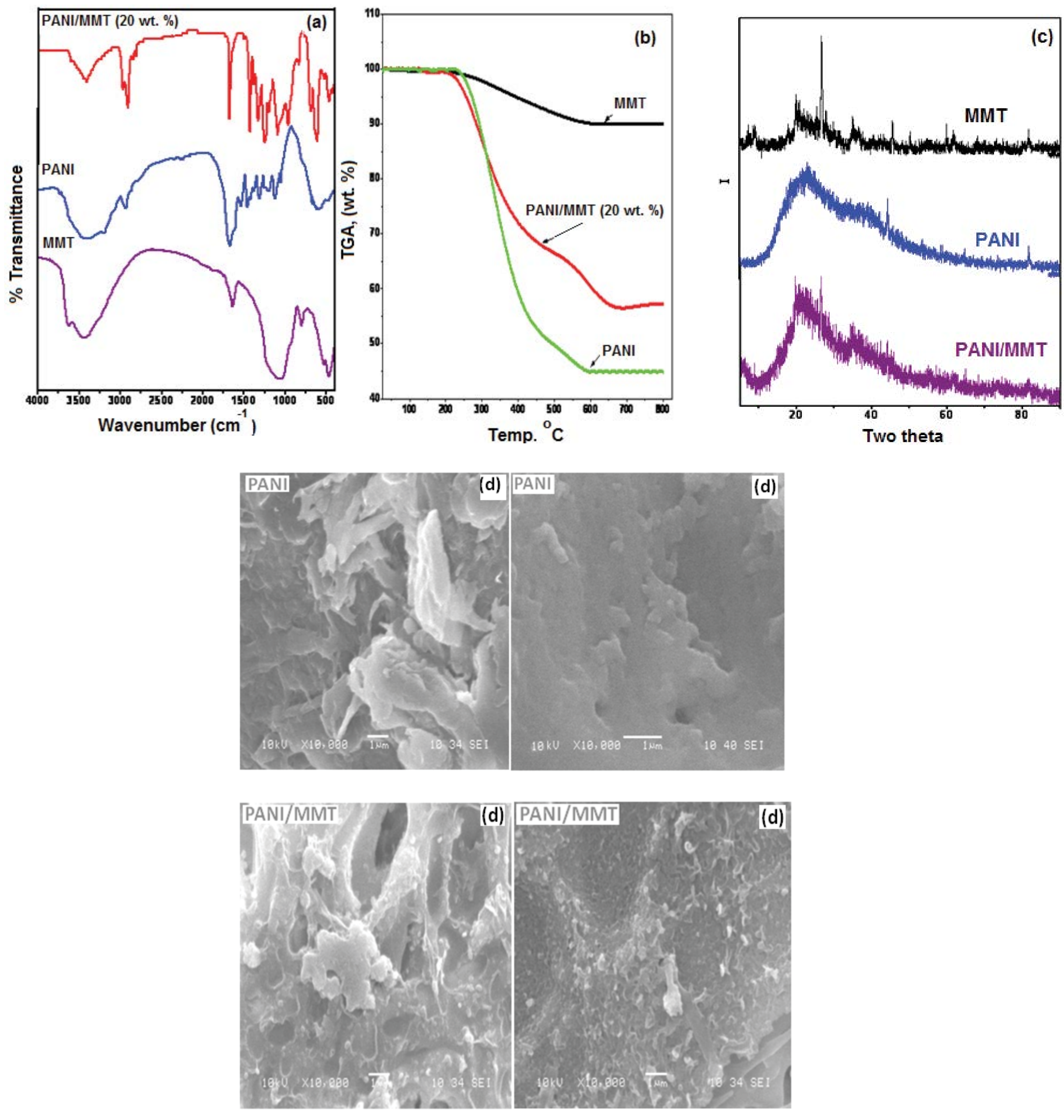

Fig. 1. FT-IR spectra (a), TGA analysis (b), XRD patterns (c) and SEM micrographs (d) for MMT, PANI, PANI/MMT.

On the other hand, at pH within 5–7, the copper ions solubility decreased and precipitate as $Cu(OH)_2$ [51]. The point of zero charge for PANI was reported to be 5.2, so the polymer surface is positively charged before pH 5.2 [52]. The presence of MMT could shift this point towards more positive due to the presence of cations within MMT.

3.2.2. *Effect of adsorbent dose*

The effect of adsorbent dose on the adsorption of Cu(II) onto PANI and PANI/MMT was studied at different dose (from 0.2 to 4 g L^{-1}), with fixing other experimental parameters. The results presented in Fig. 2b show that the residual Cu(II) concentration in solution decreased dramatically with increasing adsorbent dose of PANI and PANI/MMT up to 2 g L^{-1}. Increasing the adsorbent dose more than 2 g L^{-1} shows no corresponding increase in adsorption. The usage of high adsorbent dose without significant increase in adsorption is not economically recommended, therefore the optimum adsorbent dose was considered to be 2 g L^{-1}. The observed adsorption at higher dose than 2 g L^{-1} reflects that there were still adsorption active sites

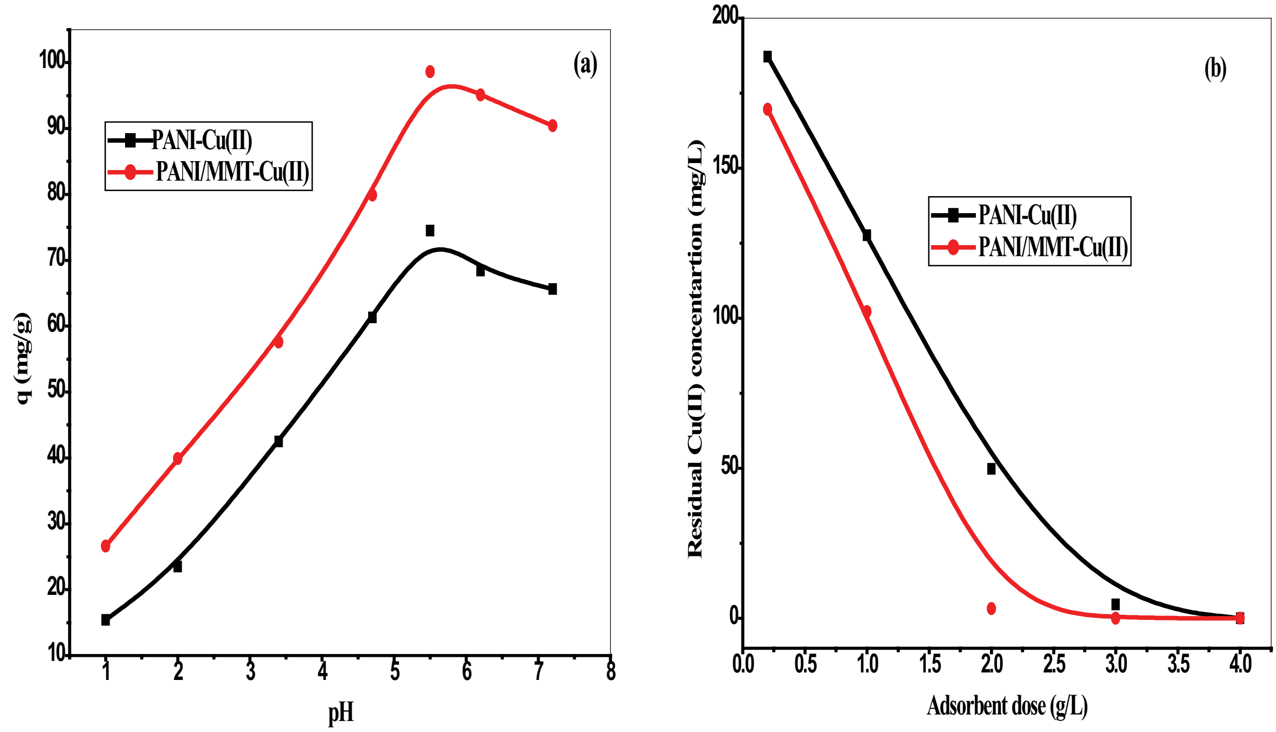

Fig. 2. Effect of pH; contact time 60 min, adsorbent dose 2 g L^{-1}, Temp. 25°C ± 1°C, Cu(II) concentration is 200 mg L^{-1} (a), effect of adsorbent dose; pH 5.5, Cu(II) concentration 200 mg L^{-1}, contact time 60 min and Temp. 25°C ± 1°C (b).

un-reacted within the adsorbent. The adsorbent active sites per gram are not all reinforced for interaction, so a regular decrease in adsorption was observed [53,54].

3.2.3. Effect of Cu(II) ion concentration and isothermal studies

The isothermal studies provide certain information about the adsorption process as the maximum adsorption capacity and provide information about adsorption mechanism. The effect of initial Cu(II) ion concentration on the equilibrium adsorbed amount was studied. The results were presented as residual equilibrium Cu(II) concentration in solution (C_e, mg L^{-1}) against the amount of Cu(II) adsorbed on the solid adsorbent (q_e, mg g^{-1}) Fig. 3a. Different isotherm models, namely Langmuir, Freundlich and Temkin were applied on the experimental results. Langmuir isotherm model explain monolayer adsorption of Cu(II) ions on the outer adsorbent surface with no more adsorption after the monolayer adsorption. The linear form of Langmuir model equation is:

$$\frac{1}{q_e} = \frac{1}{q_{\max}} + \frac{1}{bq_{\max}C_e} \tag{4}$$

where q_e and $q_{\max}$ are the adsorbed amount (mg g^{-1}) of Cu(II) ions at equilibrium and the maximum adsorbed amount (mg g^{-1}), respectively. C_e is the Cu(II) ion concentration in solution at equilibrium (mg L^{-1}) and b (L mg^{-1}) is a constant related to the adsorption free energy [55]. The model parameters were calculated from the plot of $1/q_e$ vs. $1/C_e$ (Fig. 3b) and are given in Table 1. The correlation coefficient (R^2) for Langmuir isotherm model are 0.991 and 0.983 for PANI-Cu(II) and PANI/MMT-Cu(II) adsorption systems, respectively.

Freundlich isotherm model was used to explain the adsorption on heterogeneous surfaces and given by the following equation:

$$\log q_e = \log K_f + \frac{1}{n}\log C_e \tag{5}$$

where K_f is a constant related to the adsorbed amount (mg g^{-1}) and $1/n$ is a constant related to the adsorption intensity. Freundlich isotherm model parameters with the correlation coefficient were calculated from the linear regression of the plot of $\log q_e$ against $\log C_e$ (Fig. 3c) and are given in Table 1. The values of R^2 and the K_f in Table 1 indicate a god fit of the experimental results with Langmuir model than Freundlich model.

Temkin isotherm model consider the interaction between distinctive adsorbate molecules on the adsorbent given by the equation:

$$q_e = \frac{RT}{B}\ln A + \frac{RT}{B}\ln C_e \tag{6}$$

where A (L g^{-1}) and B (J mol^{-1}) are Temkin model constants, R (J mol^{-1} K^{-1}) is the universal gas constant and T (K) is the absolute temperature. The values of A, B and R^2 were

Table 1
Isotherm model parameters for the adsorption of Cu(II) onto PANI and PANI/MMT

Ads. system	Isotherm model parameters		
	Langmuir	Freundlich	Temkin
PANI-Cu(II)	q_{max} = 85.47 mg g^{-1}	$1/n$ = 0.349	A = 1.468 L g^{-1}
	b = 0.173 L mg^{-1}	K_f = 19.54 mg g^{-1}	B = 134.81 J mol^{-1}
	R^2 = 0.991	R^2 = 0.992	R^2 = 0.992
	S.D. = 0.00186	S.D. = 0.0319	S.D. = 3.95
PANI/MMT-Cu(II)	q_{max} = 100.01 mg g^{-1}	$1/n$ = 0.256	A = 2.945 L g^{-1}
	b = 3.33 L mg^{-1}	K_f = 56.75 mg g^{-1}	B = 146.26 J mol^{-1}
	R^2 = 0.983	R^2 = 0.943	R^2 = 0.975
	S.D. = 0.0025	S.D. = 0.098	S.D. = 3.35

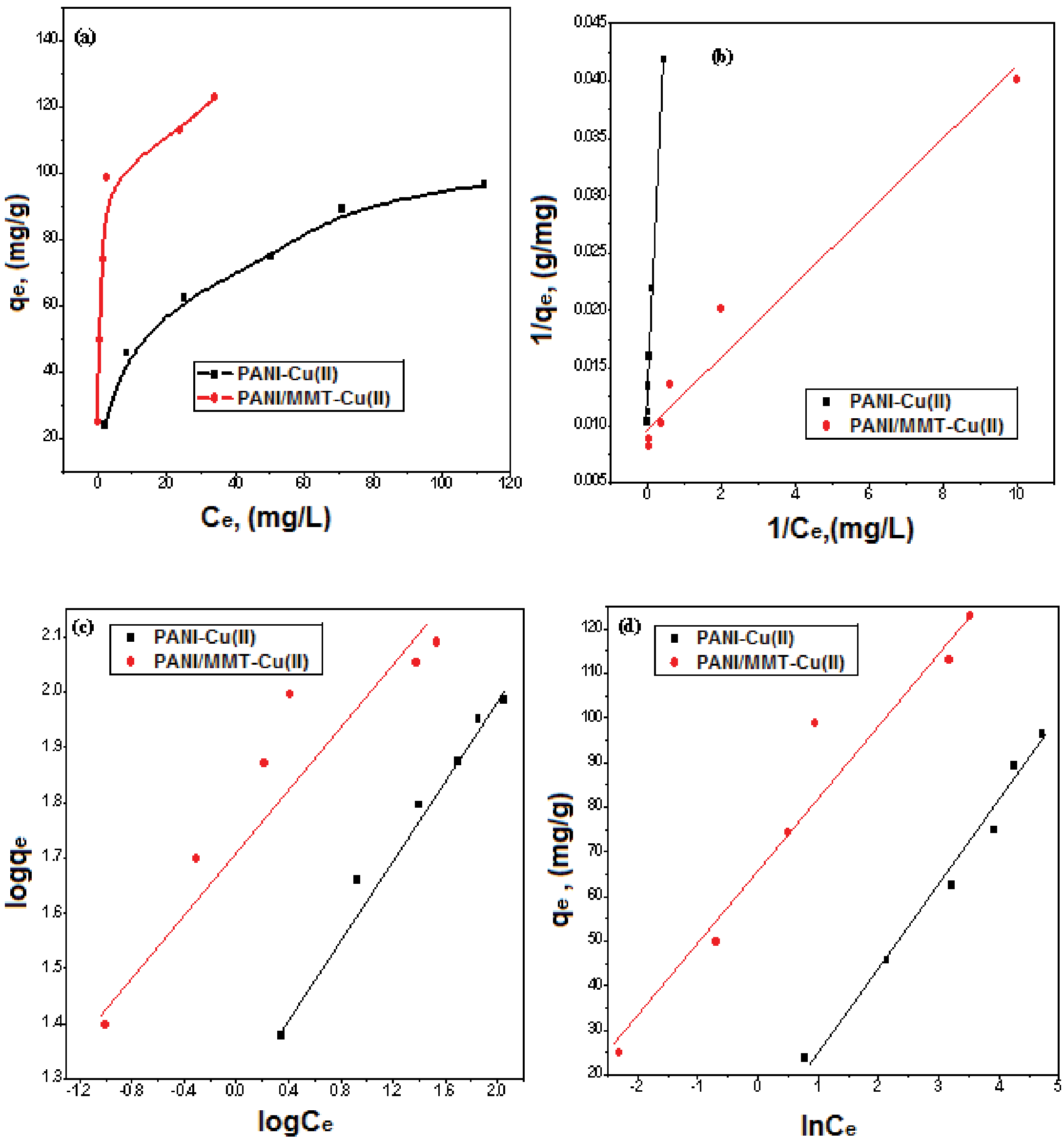

Fig. 3. Effect of Cu(II) ion concentration; dose 2 g L^{-1}, pH 5.5, time 60 min and temperature of 25°C ± 1°C (a), Langmuir model plot (b), Freundlich model plot (c) and Temkin model plot (d).

calculated from the plot of q_e against $\ln C_e$ (Fig. 3d) and are given in Table 1.

The adsorption capacity of PANI/MMT was found evidently high and relatively higher compared to PANI. The results indicate that the prepared composite adsorbent PANI/MMT could be considered as a potential adsorbent for removal of toxic metal ions from aqueous and reflect high affinity of Cu(II) ions towards PANI/MMT. The results of isothermal studies reflect the participation of both chemical and physical adsorption in the process with presence of certain adsorbate molecules interaction on the adsorbent surface.

3.2.4. Effect of contact time and kinetic studies

The effect of contact time on the adsorbed amount of Cu(II) onto either PANI and PANI/MMT was studied and the results are given in Fig. 4a. The results showed a fast increase in the adsorbed amount of Cu(II) with time and reached equilibrium after 90 min.

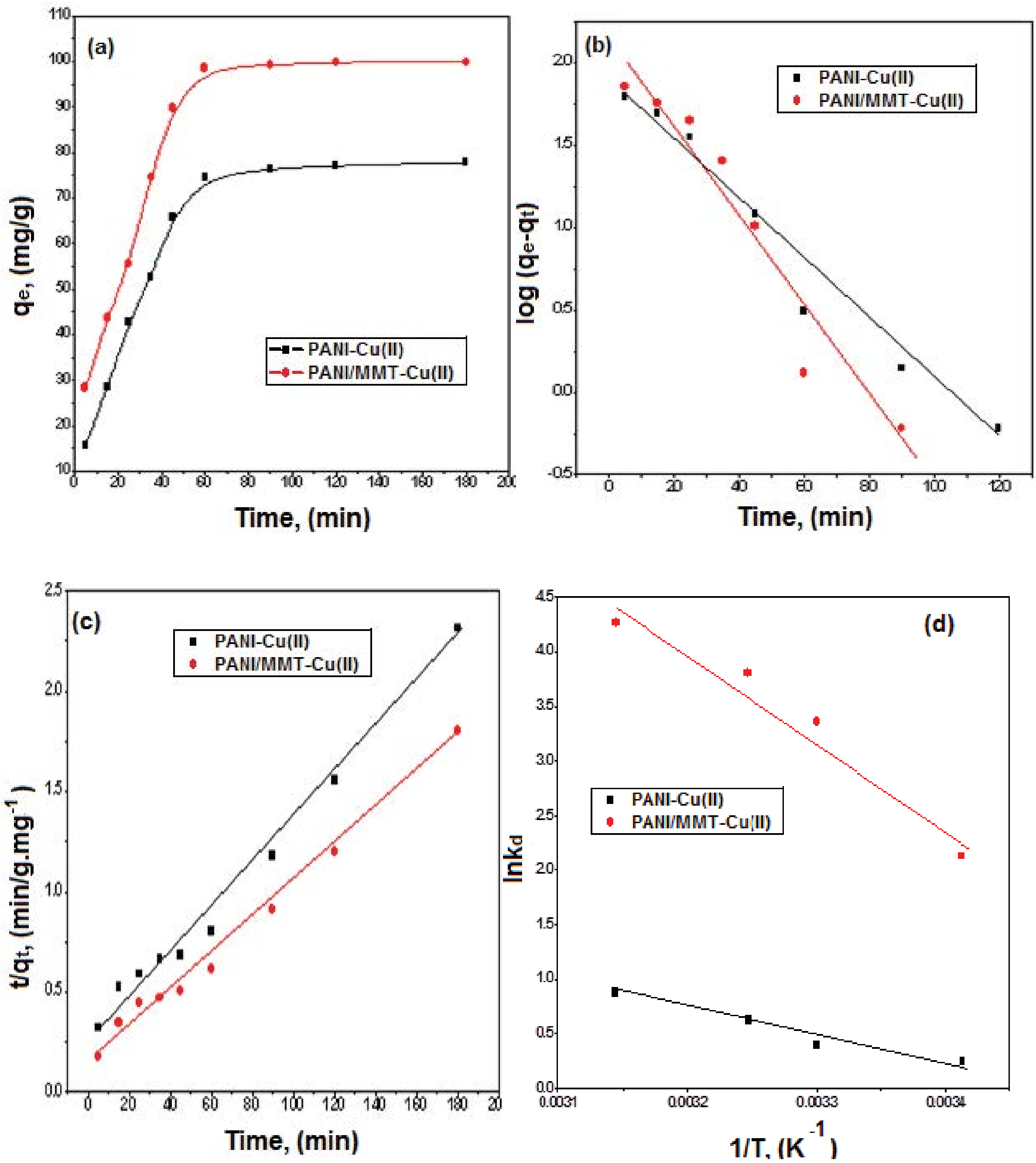

Fig. 4. Effect of contact time; dose of 2 g L^{-1}, pH 5.5, Cu(II) conc. of 200 mg L^{-1} and temperature 25°C ± 1°C (a), pseudo-first-order plot (b), pseudo-second-order plot (c) and plot of ln$k$ vs. 1/T (d).

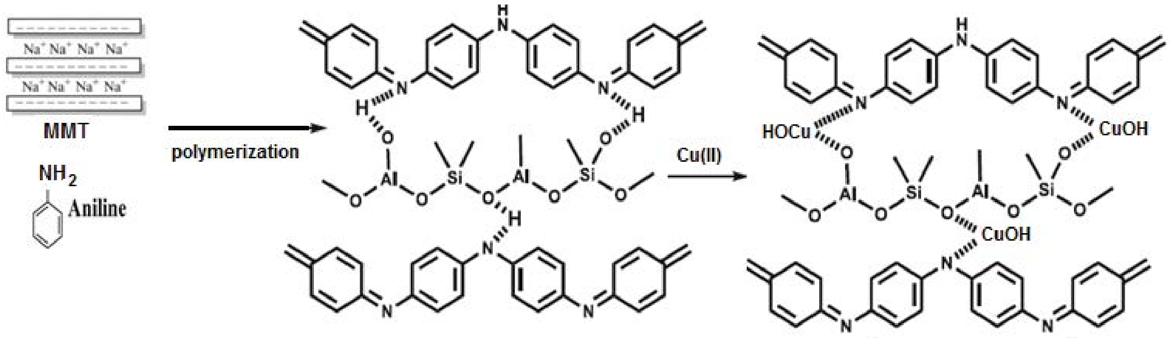

Fig. 5. The synthesis of PANI/MMT composite and Cu(II) ions adsorption.

The obtained experimental results were treated by pseudo-first-order and pseudo-second-order kinetic models. The pseudo-first-order kinetic model was presented by the following equation:

$$\log\left(q_e - q_t\right) = \log q_e - \frac{k_1 t}{2.303} \tag{7}$$

where k_1 (min^{-1}) is the rate constant of pseudo-first-order model, q_e and q_t (mg g^{-1}) are the adsorbed amount of Cu(II) at equilibrium and at time t (min), respectively. The pseudo-first-order model parameters were calculated from the plot of log($q_e - q_t$) vs. t (Fig. 4b) and are given in Table 2.

The pseudo-second-order kinetic model is presented by the equation:

$$\frac{t}{q_t} = \frac{1}{k_2 q_2^2} + \frac{t}{q_e} \tag{8}$$

where k_2 (g mg^{-1} min^{-1}) is the pseudo-second-order rate constant. The model parameters were calculated from the plot of t/q_t against t (Fig. 4c) and are listed in Table 2.

The experimental results showed god fit with the pseudo-second-order kinetic model with correlation coefficients of 0.993 and 0.995 for PANI-Cu(II) and PANI/MMT-Cu(II) systems, respectively. Furthermore, the calculated adsorption capacity from the pseudo-second-order model was found to be more close to the experimentally determined results. These observations indicate that the adsorption of Cu(II) onto either PANI/MMT or PANI follows the pseudo-second-order model, referring to the strong participation of chemical adsorption in the process [56,57].

3.2.5. Effect of temperature and adsorption thermodynamics

The effect of temperature on the adsorption of Cu(II) using PANI and PANI/MMT was studied within the temperature range (25°C–45°C). The thermodynamic parameters of the adsorption process as Gibbs free energy ΔG (kJ mol^{-1}), enthalpy change ΔH (kJ mol^{-1}), and entropy change ΔS (J mol^{-1} K^{-1}) were calculated using the following equations:

$$k = \frac{q_e}{C_e} \tag{9}$$

$$\ln k = \frac{\Delta S}{R} - \frac{\Delta H}{RT} \tag{10}$$

$$\Delta G = \Delta H - T\Delta S \tag{11}$$

where k is the equilibrium constant, T (K) is the absolute temperature and R is the gas constant (8.314 J mol^{-1} K^{-1}). The enthalpy change and entropy change were calculated from the plot of ln$k$ against 1/T (Fig. 4d) and are given in Table 3.

Table 2
Pseudo-first-order and pseudo-second-order model's parameters for PANI-Cu(II) and PANI/MMT-Cu(II) adsorption systems

Ads. system	Kinetic model parameters	
	Pseudo-first-order	Pseudo-second-order
PANI-Cu(II)	q_e = 85.11 mg g^{-1}	q_e = 91.15 mg g^{-1}
	k_1 = 0.0439 min^{-1}	k_2 = 4.65 × 10^{-4} g mg^{-1} min^{-1}
	R^2 = 0.982	R^2 = 0.993
	S.D. = 0.153	S.D. = 0.078
PANI/MMT-Cu(II)	q_e = 145.88 mg g^{-1}	q_e = 112.48 mg g^{-1}
	k_1 = 0.0635 min^{-1}	k_2 = 5.30 × 10^{-4} g mg^{-1} min^{-1}
	R^2 = 0.966	R^2 = 0.995
	S.D. = 0.233	S.D. = 0.057

The calculated thermodynamic parameters showed negative values for the free energy change Δ*G*, reflecting the feasibility and spontaneous nature of the adsorption process at room temperature. The positive values of the enthalpy changes Δ*H* refer to the endothermic nature of the adsorption of Cu(II) on either PANI or PANI/MMT. The entropy change Δ*S* showed positive values which indicate randomness at the solid liquid interface with the course of the adsorption process of Cu(II) ions onto PANI and PANI/MMT [58,59]. Based on the obtained results the suggested mechanism of composite preparation and adsorption of Cu(II) onto PANI/MMT was presented in Fig. 5.

3.3. Regeneration and reuse of adsorbent

The copper ion recycling and the recovery of the composite adsorbent is an important consideration in adsorption studies. The regeneration-recycling of the Cu(II) loaded adsorbents PANI and PANI/MMT was performed by 0.1 M HCl solution. The results showed higher desorption of Cu(II) ions from PANI/MMT using HCl solution, which could be explained due the competing effect of hydrogen ions at acidic condition. Consequently, a higher regeneration was observed by acidic solutions. The regenerated adsorbents were applied in repeated adsorption-desorption cycles up to five cycles. The results showed significant adsorption efficiency of Cu(II) ions up to the fourth cycle (with removal of 90%) with respect PANI/MMT. While, with respect to PANI, the adsorption efficiency decreased significantly after the third cycle (removal reached 72%). These observations reflect the stability of the composite adsorbent PANI/MMT for removal of Cu(II) in repeated cycles compared to PANI.

3.4. Comparining the adsosrption of Cu(II) using PANI/MMT with different adsorbents

The maximum adsorbed amount of Cu(II) using the prepared composite PANI/MMT is presented in Table 4 with the maximum adsoebed amount of Cu(II) using different adosrbets. The data in Table 4 show that PANI/MMT composite has a potential adsorption efficiny if comapred with different adsorbents. The results encorage future studies for adsorption of other heavy metal and/or organic pollutants from wastewater using the prepared composite PANI/MMT composite.

4. Conclusion

In the present study polyaniline and polyaniline/montmorillonite composite adsorbents were prepared and studied for the removal of copper(II) ions from aqueous solutions. The composite adsorbent PANI/MMT showed higher adsorption capacity for Cu(II) ions than PANI and showed high affinity for Cu(II) ions. The pH of higher adsorption is 5.5 and the equilibrium reached after 90 min with adsorption capacity of 99.61 mg g^{-1} with respect to PANI/MMT. The isothermal and kinetic studies showed god fit of the experimental results of Cu(II) adsorption by PANI or PANI/MMT with Langmuir isotherm model and pseudo-second-order kinetic model. The calculated maximum adsorption capacity of Cu(II) was found to be 100.01 mg g^{-1}. The thermodynamic study showed endothermic, spontaneous and feasible adsorption process. Furthermore, PANI/MMT could be easily regenerated using acidic solution and reused up to four cycles with significant adsorption efficiency and particles stability. The composite PANI/MMT could be considered as an efficient adsorbent to remove Cu(II) ions from aqueous solution and could be applied for removal of other metal ions as well. Based on the obtained results, we recommend the application of the prepared composite PANI/MMT for removal other pollutants in future work.

Acknowledgment

The authors extend their appreciation to the Deanship of Scientific Research at King Khalid University for funding

Table 3
Thermodynamic parameters for the adsorption of Cu(II) onto PANI and PANI/MMT

Thermodynamic parameters	PANI-Cu(II)	PANI/MMT-Cu(II)
Δ*H* (kJ mol^{-1})	20.28	66.50
Δ*G* (kJ mol^{-1})	–0.843	–6.80
Δ*S* (J mol^{-1} K^{-1})	70.88	246.01

Table 4
Maximum adsorbed amount of Cu(II) by different adsorbents

Adsorbent	Maximum adsorption, (mg g^{-1})	Adsorption model	References
Sodium alginate modified materials	5.6	Langmuir	[60]
Waste tire rubber ash	34.3	Langmuir	[61]
Chemically modified bioadsorbents	92.5	Langmuir	[62]
Bagasse pith grafted polyacrylamide copolymer	105.3	Langmuir	[63]
PANI/MMT	100.01	Langmuir	Current study

this work through research groups program under grant number R.G.P. 1/230/41.

References

[1] A. Shokuhfar, A. Zare-Shahabadi, A.-A. Atai, S. Ebrahimi-Nejad, M. Termeh, Predictive modeling of creep in polymer/layered silicate nanocomposites, Polym. Test., 31 (2012) 345–354.

[2] P. Kiliaris, C.D. Papaspyrides, Polymer/layered silicate (clay) nanocomposites: an overview of flame retardancy, Prog. Polym. Sci., 35 (2010) 902–958.

[3] F. Uddin, Montmorillonite: An Introduction to Properties and Utilization, M. Zoveidavianpoor, Ed., Current Topics in the Utilization of Clay in Industrial and Medical Applications, IntechOpen, 2018, p. 3:23, doi: 10.5772/intechopen.77987. Available at: https://www.intechopen.com/chapters/61845

[4] N.P. Shetti, D.S. Nayak, K.R Reddy and T.M. Aminabihavi, Chapter 10 – Graphene–Clay-Based Hybrid Nanostructures for Electrochemical Sensors and Biosensors, A. Pandikumar, P. Rameshkumar, Eds., Graphene-Based Electrochemical Sensors for Biomolecules: Micro and Nano Technologies, Elsevier, Radarweg 29, P.O. Box: 211, 1000 AE Amsterdam, Netherlands, 2019, pp. 235–274.

[5] K.G. Bhattacharyya, S.S. Gupta, Adsorption of a few heavy metals on natural and modified kaolinite and montmorillonite: a review, Adv. Colloid Interface Sci., 140 (2008) 114–131.

[6] M. Auta, B.H. Hameed, Chitosan–clay composite as highly effective and low-cost adsorbent for batch and fixed-bed adsorption of methylene blue, Chem. Eng. J., 237 (2014) 352–361.

[7] Md. R. Awual, M. Ismael, T. Yaita, S.A. El-Safty, H. Shiwaku, Y. Okamoto, S. Suzuki, Trace copper(II) ions detection and removal from water using novel ligand modified composite adsorbent, Chem. Eng. J., 222 (2013) 67–76.

[8] M. Auta, B.H. Hameed, Coalesced chitosan activated carbon composite for batch and fixed-bed adsorption of cationic and anionic dyes, Colloids Surf., B, 105 (2013) 199–206.

[9] R.-S. Norouzian, M.M. Lakouraj, Preparation and heavy metal ion adsorption behavior of novel supermagnetic nanocomposite of hydrophilic thiacalix[4]arene self-doped polyaniline: conductivity, isotherm, and kinetic study, Adv. Polym. Technol., 36 (2017) 107–119.

[10] N.M. Ismail, A.F. Ismail, A. Mustafa, T. Matsuura, T. Soga, K. Nagata, T. Asaka, Qualitative and quantitative analysis of intercalated and exfoliated silicate layers in asymmetric polyethersulfone/cloisite15A® mixed matrix membrane for CO_2/CH_4 separation, Chem. Eng. J., 268 (2015) 371–383.

[11] E.F. Unuabonah, A. Taubert, Clay–polymer nanocomposites (CPNs): adsorbents of the future for water treatment, Appl. Clay Sci., 99 (2014) 83–92.

[12] Y. Zou, X. Wang, A. Khan, P. Wang, Y. Liu, A. Alsaedi, T. Hayat, X. Wang, Environmental remediation and application of nanoscale zero-valent iron and its composites for the removal of heavy metal ions: a review, Environ. Sci. Technol. – ACS, 50 (2016) 7290–7304.

[13] S. Sharaf, A. Aslam, M. Rabbani, A. Sharf, M. Ijaz, A. Anjum, N. Hussain, Toxico-pathological effects of heavy metals from industrial drainage wastewater on vital organs of small ruminants in Lahore, Environ. Sci. Pollut. Res., 28 (2020) 3533–3543.

[14] I. García-Díaz, F.A. López, F.J. Alguaci, Carbon nanofibers: a new adsorbent for copper removal from wastewater, Metals (Basel), 8 (2018) 914–927.

[15] J. Mishra, R. Saini, D. Singh, Review paper on removal of heavy metal ions from industrial waste water effluent, IOP Conf. Ser.: Mater. Sci. Eng., 1168 (2021) 012027.

[16] S.A. Al-Saydeh, M.H. El-Naas, S.J. Zaidi, Copper removal from industrial wastewater: a comprehensive review, J. Ind. Eng. Chem., 56 (2017) 35–44.

[17] H. Aydın, Y. Bulut, C. Yerlikaya, Removal of copper(II) from aqueous solution by adsorption onto low-cost adsorbents, J. Environ. Manage., 87 (2008) 37–45.

[18] S. Andrejkovičová, A. Sudagar, J. Rocha, C. Patinha, W. Hajjaji, E. Ferreira da Silva, A. Velosa, A. Rocha, The effect of natural zeolite on microstructure, mechanical and heavy metals adsorption properties of metakaolin based geopolymers, Appl. Clay Sci., 126 (2016) 141–152.

[19] O. Ferrer, O. Gibert, J.L. Cortina, Reverse osmosis membrane composition, structure and performance modification by bisulphite, iron(III), bromide and chlorite exposure, Water Res., 103 (2016) 256–263.

[20] Y.C. Xu, Z.X. Wang, X.Q. Cheng, Y.C. Xiao, L. Shao, Positively charged nanofiltration membranes via economically mussel-substance-simulated co-deposition for textile wastewater treatment, Chem. Eng. J., 303 (2016) 555–564.

[21] Y. Dong, J. Liu, M. Sui, Y. Qu, J.J. Ambuchi, H. Wang, Y. Feng, A combined microbial desalination cell and electrodialysis system for copper-containing wastewater treatment and high-salinity-water desalination, J. Hazard. Mater., 321 (2017) 307–315.

[22] D. Kanakaraju, S. Ravichandar, Y.C. Lim, Combined effects of adsorption and photocatalysis by hybrid TiO_2/ZnO-calcium alginate beads for the removal of copper, J. Environ. Sci., 55 (2017) 214–223.

[23] R. Davarnejad, P. Panahi, Cu(II) removal from aqueous wastewaters by adsorption on the modified Henna with Fe_3O_4 nanoparticles using response surface methodology, Sep. Purif. Technol., 158 (2016) 286–262.

[24] N.B. Hafizah, Adsorption of copper(II) from aqueous solution using tea (*Camellia sinensis*) leaf waste, Mater. Sci. Forum, 997 (2020) 113–120.

[25] S.S. Al Moharbi, M. Geetha Devi, B.M. Sangeetha, S. Jahan, Studies on the removal of copper ions from industrial effluent by *Azadirachta indica* powder, Appl. Water Sci., 10 (2020) 23, doi: 10.1007/s13201-019-1100-z.

[26] N.E. Dávila-Guzmán, Y.B. Medina-Almaguer, M.A. Reyes-González, M. Loredo-Cancino, S. Pioquinto-García, D.A. De Haro-Del Rio, M.A. Garza-Navarro, E. Hernández-Fernández, Microwave-assisted synthesis of *trans*-cinnamic acid for highly efficient removal of copper from aqueous solution, ACS Omega, 5 (2020) 317–326.

[27] M. Moubarek, H. Kadda, H.M. Kaid, Lignocellulosic fraction of the pericarps of the acorns of *Quercus suber* and *Quercus ilex*: isolation, characterization, and biosorption studies in the removal of copper from aqueous solutions, Pol. J. Chem. Technol., 21 (2019) 40–47.

[28] R.O. Adeeyo, J.N. Edokpayi, O.S. Bello, A.O. Adeeyo, J.O. Odiyo, Influence of selective conditions on various composite sorbents for enhanced removal of copper(II) ions from aqueous environments, Int. J. Environ. Res., 16 (2019) 4596–4613.

[29] R. Ansari, Application of polyaniline and its composites for adsorption/recovery of chromium(VI) from aqueous solutions, Acta Chim. Slov., 53 (2006) 88–94.

[30] S. Raja, M. Deepa, Synthesis and characterization of polyaniline-copper(II) oxide nanocomposite by wet chemical route, Indian J. Adv. Chem. Sci., 3 (2015) 198–203.

[31] V. Babel, B.L. Hiran, A review on polyaniline composites: synthesis, characterization, and applications, Polym. Compos., 42 (2021) 3142–3157.

[32] H. Hajjaoui, A. Soufi, W. Boumya, M. Abdennouri, N. Barka, Polyaniline/nanomaterial composites for the removal of heavy metals by adsorption: a review, J. Compos. Sci., 5 (2021) 233–255.

[33] K. Rajakumar, S. Dinesh Kirupha, S. Sivanesan, R.L. Sai, Effective removal of heavy metal ions using Mn_2O_3 doped polyaniline nanocomposite, J. Nanosci. Nanotechnol., 14 (2014) 2937–2946.

[34] R. Khalili, H. Eisazadeh, Preparation and characterization of polyaniline/Sb_2O_3 nanocomposite and its application for removal of Pb(II) from aqueous media, Int. J. Eng., 27 (2013) 239–246.

[35] S. Piri, F. Piri, B. Rajabi, S. Ebrahimi, A. Zamani, M.R. Yaftian, In situ one-pot electrochemical synthesis of aluminum oxide/polyaniline nanocomposite; characterization and its adsorption properties towards some heavy metal ions, J. Chin. Chem. Soc., 62 (2015) 1045–1052.

[36] A. Hsini, A. Essekri, N. Aarab, M. Laabd, A.A. Addi, R. Lakhmiri, A. Albourine, Elaboration of novel polyaniline@ Almond shell biocomposite for effective removal of hexavalent chromium ions and Orange G dye from aqueous solutions, Environ. Sci. Pollut. Res., 27 (2020) 15245–15258.

[37] S. Majumdar, A. Baishya, D. Mahanta, Kinetic and equilibrium modeling of anionic dye adsorption on polyaniline emeraldine salt: batch and fixed bed column studies, Fibers Polym., 20 (2019) 1226–1235.

[38] M. Laabd, H. Chafai, A. Essekri, M. Elamine, S.A. Al-Muhtaseb, R. Lakhmiri, A. Albourine, Single and multi-component adsorption of aromatic acids using an eco-friendly polyaniline-based biocomposite, Sustainable Mater. Technol., 12 (2017) 35–43.

[39] L. Sun, L. Zhan, Y. Shi, L. Chu, G. Ge, Z. He, Microemulsion synthesis and electromagnetic wave absorption properties of monodispersed Fe_3O_4/polyaniline core–shell nanocomposites, Synth. Met., 187 (2014) 102–107.

[40] H. Guo, H. Zhu, H. Lin, J. Zhang, Synthesis of polyaniline/multi-walled carbon nanotube nanocomposites in water/oil microemulsion, Mater. Lett., 62 (2008) 3919–3921.

[41] M.R. Karim, H.W. Lee, I.W. Cheong, S.M. Park, W. Oh, J.H. Yeum, Conducting polyaniline-titanium dioxide nanocomposites prepared by inverted emulsion polymerization, Polym. Polym. Compos., 31 (2008) 83–88.

[42] R. Regueira, R.Y. Suckeveriene, I. Brook, G. Mechrez, R. Tchoudakov, M. Narkis, Investigation of the electro-mechanical behavior of hybrid polyaniline/graphene nano-composites fabricated by dynamic interfacial inverse emulsion polymerization, Graphene, 4 (2015) 7–19.

[43] N. Wang, J. Chen, J. Wang, J. Feng, W. Yan, Removal of methylene blue by polyaniline/TiO_2 hydrate: adsorption kinetic, isotherm and mechanism studies, Powder Technol., 347 (2019) 93–102.

[44] P. Piromruen, S. Kongparakul, P. Prasassarakich, Synthesis of polyaniline/montmorillonite nanocomposites with an enhanced anticorrosive performance, Prog. Org. Coat., 77 (2014) 691–700.

[45] H.S. Nalwa, Conductive Polymers: Synthesis and Electrical Properties, West Sussex England, John Wiley & Sons, 1997.

[46] Y.D. Liu, F.F. Fang, H.J. Choi and Y. Seo, Fabrication of semiconducting polyaniline/nano-silica nanocomposite particles and their enhanced electrorheological and dielectric characteristics, Colloids Surf., A, 381 (2011) 17–22.

[47] B.N. Narayanan, R. Koodathil, T. Gangadharan, Z. Yaakob, F.K. Saidu, S. Chandralayam, Preparation and characterization of exfoliated polyaniline/montmorillonite nanocomposites, Mater. Sci. Eng., B, 168 (2010) 242–244.

[48] T.J. Pinnavaia, G.W. Beall, Polymer-Clay Nanocomposites, John Wiley & Sons, West Sussex-England, 2000.

[49] Q.Y. Soundararajah, B.S.B. Karunarathne, R.M.G. Rajapakse, Montmorillonite polyaniline nanocomposites: preparation, characterization and investigation of mechanical properties, Mater. Chem. Phys., 113 (2009) 850–855.

[50] G. Thakur, A. Singh, I. Singh, Chitosan-montmorillonite polymer composites: formulation and evaluation of sustained release tablets of aceclofenac, Sci. Pharm., 84 (2015) 603–618.

[51] J. Alam, A.K. Shukla, M.A. Ansari, F.A. Ahmed Ali, M. Alhoshan, Dye separation and antibacterial activities of polyaniline thin film-coated poly(phenyl sulfone) membranes, Membranes, 11 (2021) 25–32.

[52] T.S. Anirudhan, S.P. Suchithra, Heavy metals uptake from aqueous solutions and industrial wastewaters by humic acid-immobilized polymer/bentonite composite: kinetics and equilibrium modeling, Chem. Eng. J., 156 (2010) 146–156.

[53] M. Helen Kalavathy, L.R. Miranda, *Moringa oleifera*—a solid phase extractant for the removal of copper, nickel and zinc from aqueous solutions, Chem. Eng. J., 158 (2010) 188–199.

[54] K. Swayampakula, V.M. Boddu, S.K. Nadavala, K. Abburi, Competitive adsorption of Cu(II), Co(II) and Ni(II) from their binary and tertiary aqueous solutions using chitosan-coated perlite beads as biosorbent, J. Hazard. Mater., 170 (2009) 680–689.

[55] V.B.H. Dang, H.D. Doan, T. Dang-Vu, A. Lohi, Equilibrium and kinetics of biosorption of cadmium(II) and copper(II) ions by wheat straw, Bioresour. Technol., 100 (2009) 211–219.

[56] A. Masoumi, M. Ghaemy, A.N. Bakht, Removal of metal ions from water using poly(MMA-*co*-MA)/modified-Fe_3O_4 magnetic nanocomposite: isotherm and kinetic study, Ind. Eng. Chem. Res. – ACS, 53 (2014) 8188–8197.

[57] Y. Xu, Z. Hao, H. Chen, J. Sun, D. Wang, Preparation of polyacrylonitrile initiated by modified corn starch and adsorption for mercury after modification, Ind. Eng. Chem. Res. – ACS, 53 (2014) 4871–4877.

[58] H.-T. Fan, X.-T. Sun, Z.-G. Zhang, W.-X. Li, Selective removal of lead(II) from aqueous solution by an ion-imprinted silica sorbent functionalized with chelating N-donor atoms, J. Chem. Eng. Data, 59 (2014) 2106–2114.

[59] M. Boroumand Jazi, M. Arshadi, M.J. Amiri, A. Gil, Kinetic and thermodynamic investigations of Pb(II) and Cd(II) adsorption on nanoscale organo-functionalized SiO_2-Al_2O_3, J. Colloid Interface Sci., 422 (2014) 16–24.

[60] Y. Zhao, L. Zhan, Z. Xue, K.K. Yusef, H. Hu, M. Wu, Adsorption of Cu(II) and Cd(II) from wastewater by sodium alginate modified materials, J. Chem., 2020 (2020) 5496712, doi: 10.1155/2020/5496712.

[61] H.Z. Mousavi, A. Hosseinifar, V. Jahed, Removal of Cu(II) from wastewater by waste tire rubber ash, J. Serb. Chem. Soc., 75 (2010) 845–853.

[62] P. Phuengphai, T. Singjanusong, N. Kheangkhun, A. Wattana-kornsiri, Removal of copper(II) from aqueous solution using chemically modified fruit peels as efficient low-cost biosorbents, Water Sci. Eng., 14 (2021) 286–294.

[63] J. Shen, K. Li, Y. Muhammad, N. Zhang, X. Guo, S. Subhan, C. Lan, K. Liu, F. Huang, Removal of Cu(II) ions from simulated wastewater using bagasse pith grafted polyacrylamide copolymer, Chem. Eng. Res. Des., 164 (2020) 361–372.